Eur. Phys. J. A **12**, 147–154 (2001)

THE EUROPEAN PHYSICAL JOURNAL A

Latest results from the HEIDELBERG-MOSCOW double beta decay experiment

H.V. Klapdor-Kleingrothaus[1,a], A. Dietz[1], L. Baudis[1], G. Heusser[1], I.V. Krivosheina[1], B. Majorovits[1], H. Paes[1], H. Strecker[1], V. Alexeev[2], A. Balysh[2], A. Bakalyarov[2], S.T. Belyaev[2], V.I. Lebedev[2], and S. Zhukov[2]

[1] Max-Planck-Institute für Kernphysik, Postfach 10 39 80, D-69029 Heidelberg, Germany
[2] Russian Science Centre, Kurchatov Institute, 123 182 Moscow, Russia

Received: 22 August 2001
Communicated by D. Schwalm

Abstract. New results for the double beta decay of ^{76}Ge are presented. They are extracted from data obtained with the HEIDELBERG-MOSCOW experiment, which operates five enriched ^{76}Ge detectors in an extreme low-level environment in the Gran Sasso underground laboratory. The two-neutrino–accompanied double beta decay is evaluated for the first time for all five detectors with a statistical significance of 47.7 kg y resulting in a half-life of $T^{2\nu}_{1/2} = [1.55 \pm 0.01(\text{stat})\,^{+0.19}_{-0.15}(\text{syst})] \times 10^{21}$ y. The lower limit on the half-life of the $0\nu\beta\beta$ decay obtained with pulse shape analysis is $T^{0\nu}_{1/2} > 1.9 \times 10^{25}$ (3.1×10^{25}) y with 90% C.L. (68% C.L.) (with 35.5 kg y). This results in an upper limit of the effective Majorana-neutrino mass of 0.35 eV (0.27 eV) using the matrix elements of A. Staudt *et al.*'s work (Europhys. Lett. **13**, 31 (1990)). This is the most stringent limit at present from double beta decay. No evidence for a majoron-emitting decay mode is observed.

PACS. 14.60.Pq Neutrino mass and mixing – 23.40.Bw Weak-interaction and lepton (including neutrino) aspects – 23.40.-s Beta decay; double beta decay; electron and muon capture – 12.60.Jv Supersymmetric models

1 Double beta decay

There seems to be a general consensus over the neutrino oscillation interpretation of the atmospheric and solar neutrino data, delivering a strong indication for a non-vanishing neutrino mass. While such kind of experiments yields information on the difference of squared neutrino mass eigenvalues and on mixing angles, the absolute scale of the neutrino mass is still unknown. Information from double beta decay experiments is indispensible to solve these questions [1–4]. Another important problem is that of the fundamental character of the neutrino, whether it is a Dirac or a Majorana particle. Neutrinoless double beta decay could answer also this question. The HEIDELBERG-MOSCOW experiment is giving, since almost eight years now, the most sensitive limit of all $\beta\beta$ experiments worldwide [4]. Double beta decay, the rarest known nuclear decay process, can occur in different modes:

$2\nu\beta\beta$ decay:

$$A(Z,N) \rightarrow A(Z+2,N-2) + 2e^- + 2\bar{\nu}_e\,, \qquad (1)$$

$0\nu\beta\beta$ decay:

$$A(Z,N) \rightarrow A(Z+2,N-2) + 2e^-\,, \qquad (2)$$

$0\nu(2)\chi\beta\beta$ decay:

$$A(Z,N) \rightarrow A(Z+2,N-2) + 2e^- + (2)\chi\,. \qquad (3)$$

The two-neutrino decay mode (1) is a conventional second-order weak process, allowed in the standard model of particle physics. So far it has been observed for about 10 different nuclei [3–5]. An accurate measurement of the half-life of the decay is of importance, since it provides a cross-check on the reliability of matrix element calculations. The majoron-emitting decay mode (3) could reveal the existence of light or massless bosons, so-called majorons, with a non-zero coupling to neutrinos. The neutrinoless mode (2) is by far the most exciting one due to the violation of the lepton number conservation by two units. It can not only probe a Majorana-neutrino mass, but various new physics scenarios beyond the standard model, such as R-parity violating supersymmetric models [6], R-parity conserving SUSY models [7], leptoquarks [8], violation of Lorentz-invariance [9] and compositeness [10] (for a review see [4,11–13]). Any theory containing lepton number violating interactions can in principle lead to

[a] e-mail: klapdor@gustav.mpi-hd.mpg.de.
Spokesman of HEIDELBERG-MOSCOW and GENIUS Collaborations. Home Page Heidelberg Non-Accelerator Particle Physics group: http://mpi-hd.mpg.de.non_acc/.

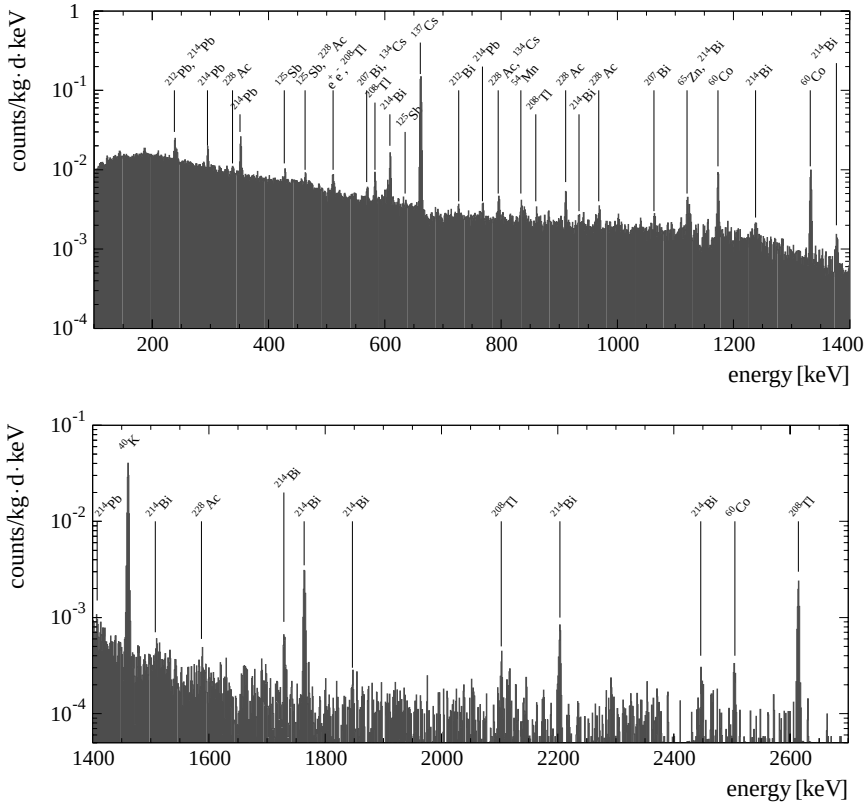

Fig. 1. Sum spectrum of all five ^{76}Ge detectors after 47.4 kg y of measurement. The most prominent identified lines are labeled.

this process allowing to obtain information on the specific underlying theory. The experimental signature of the neutrinoless mode is a peak at the Q-value of the decay, whereas for the two-neutrino and majoron-accompanied decay modes well-defined continuous energy spectra are expected. They are identified by their spectral index n, defined as the power of the energy in the phase space integral (see [14]). The majoron-emitting modes are characterized by $n = 1, 3, 7$, while for the $2\nu\beta\beta$ decay, $n = 5$.

2 The HEIDELBERG-MOSCOW experiment

The HEIDELBERG-MOSCOW experiment operates five p-type HPGe detectors in the Gran Sasso underground laboratory which were originally grown from 19.2 kg of enriched ^{76}Ge. The total active mass of the detectors is 10.96 kg, corresponding to 125.5 mol of ^{76}Ge, the presently largest source strength of all double beta experiments. The enrichment of the used Germanium is 86%. A detailed description of the experiment is given in [15].

To check the stability of the experiment, a couple of parameters such as temperature, nitrogen flow, leakage current of the detectors, overall and individual trigger rates are monitored daily. An energy calibration is done weekly with a ^{228}Th and a ^{152}Eu-^{228}Th source. The energy resolution of the detectors at 2614 keV ranges from 3–3.7 keV. The energy thresholds for data recording are set to about 70 keV (with exception of the second detector, which is used for dark matter measurements in addition, see [16]).

Figure 1 shows the combined sum spectrum of all five enriched detectors of the HEIDELBERG-MOSCOW experiment with a statistical significance of 47.4 kg y (see [17]). The large peak-to-Compton ratio of the detectors facilitates the identification of γ activities. The easily identified background components consist of primordial activities of the natural decay chains from ^{238}U and ^{232}Th, from ^{40}K, anthropogenic radionuclides, like ^{137}Cs, ^{134}Cs, ^{125}Sb and ^{207}Bi and cosmogenic isotopes, such as ^{54}Mn, ^{57}Co, ^{58}Co, ^{60}Co and ^{65}Zn. Hidden in the continuous background are the contributions of the bremsstrahlung spectrum of ^{210}Bi (daughter of ^{210}Pb), elastic and inelastic neutron scattering and direct muon-induced events.

3 Background model

The evaluation of the spectra caused by the $2\nu\beta\beta$ decay and the majoron-emitting decay modes require a detailed knowledge of the composition of the background on which they are superimposed. To unfold the background, a Monte Carlo simulation was performed. It is based on the CERN code GEANT3.21, modified for simulating radioactive decays with the complete implemented decay schemes taken from [18]. Five parts of the experimental setup have been identified to represent the main locations

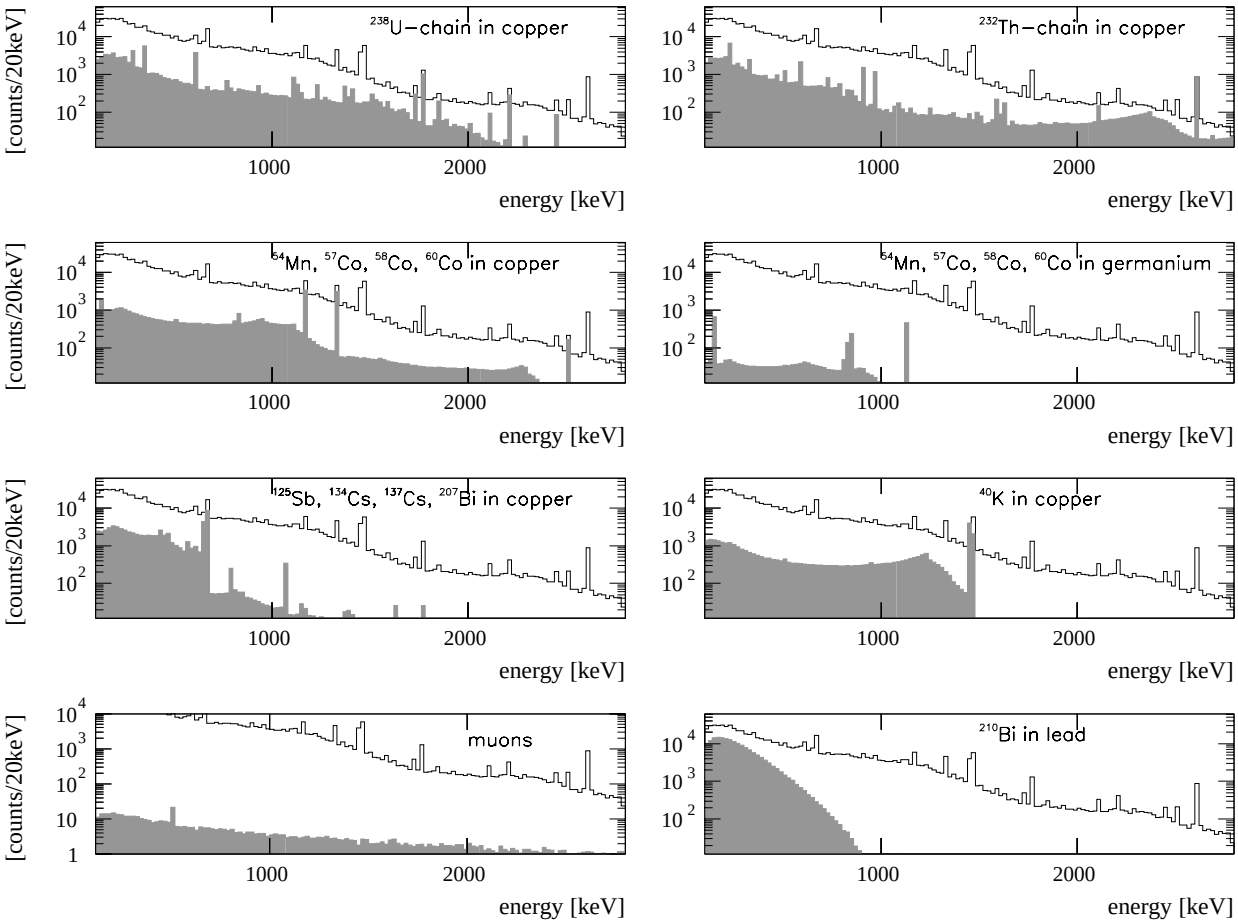

Fig. 2. The simulated background components (shaded areas) compared with the original measured sum spectrum for all five detectors.

of the radioactive impurities: the LC2-Pb shield, the copper shield, the copper and plastic parts of the cryostats and the Ge crystals themselves. Other materials or locations in the detector array are negligible due their small masses and low activities. The following background components were simulated: the natural decay chains of ^{238}U and ^{232}Th, ^{40}K, cosmogenic and anthropogenic isotopes, muon showers and neutron-induced interactions. It was assumed that the ^{238}U and ^{232}Th decay chains are in secular equilibrium and that the radioactive isotopes in the respective materials are uniformly distributed. Muon-induced showers were simulated based on the measured flux and energy distribution of muons in the Gran Sasso underground laboratory [19]. Not considered were muon-induced neutrons in the detector shielding materials, due to still large uncertainties in the absolute n-flux determinations in GEANT3.21. This component belongs to the non-identified background which will be discussed below. The measured neutron flux in the Gran Sasso underground laboratory [20] was simulated using the MICAP implementation in GEANT [21]. The activities of ^{40}K and ^{210}Pb in the LC2-Pb shield were determined in separate activity measurements [22]. In order to extract the best fit values for each activity, a least-squares method has been used. The location of the radioactive impurities was determined by comparing the peak intensities of multiline isotopes with the simulation. The error of a possible misplacement is part of the systematic error of the background model. The influence of each radioactive impurity located in one detector on all other detectors was considered. We identified a total number of 142 lines in the spectra of the five enriched Ge detectors. Their measured intensities were used to normalize the simulated components of the background model. Table 1 shows the identified background components, their estimated activities and their most probable locations in the experimental setup. The main background sources (natural decay chains, cosmogenics and anthropogenic radionuclides) were located in the copper parts of the cryostats. In the Ge crystals themselves, only cosmogenic radionuclides were identified. There is no intrinsic U/Th contamination of the crystals, due to the absence of α peaks in their high-energy spectra (the single α line at 5.3 MeV detected in two of the five detectors originates most likely from surface contaminations at the inner contact). External α and β activities are shielded by the about 0.7 mm inactive zone of the p-type detectors on the outer crystal surface. Figure 2 shows the contribution of the simulated background components in the original measured sum spectrum of the Ge detectors (for details of the simulations see [17]).

Table 1. Identified background components (primordial, cosmogenic, anthropogenic), their estimated activities and most probable locations in the full setup of the HEIDELBERG-MOSCOW experiment.

Isotope	Average for all 5 detectors	
	Localisation	Activity (μBq/kg)
^{238}U	Cu cryostat	85.0
^{238}U	Pb shield	< 11.3
^{232}Th	Cu cryostat	62.5
^{232}Th	Pb shield	< 0.9
^{40}K	Cu cryostat	480.3
^{40}K	LC2-Pb	310 (external measurement)
^{210}Pb	LC2-Pb	3.6×10^5 (external measurement)
^{54}Mn	Ge crystal	4.2
^{57}Co	Ge crystal	2.6
^{58}Co	Ge crystal	3.4 (only No. 3 & 5)
^{65}Zn	Ge crystal	20.2 (No. 2-4)
^{54}Mn	Cu cryostat	17.1
^{57}Co	Cu cryostat	32.4
^{58}Co	Cu cryostat	23.4 (only No. 3-5)
^{60}Co	Cu cryostat	65.2
^{125}Sb	Cu cryostat	36.2
^{134}Cs	Cu cryostat	5.1
^{137}Cs	Cu cryostat	67.8 (No. 5: 463.9)
^{207}Bi	Cu cryostat	7.2

4 Results for the $2\nu\beta\beta$ and the $0\nu(\chi)\chi\beta\beta$ decays

In fig. 3 the summed data of the five detectors are shown together with the result after subtracting the identified background components. A bin width of 20 keV is chosen in order to avoid statistical fluctuations when subtracting the simulated γ lines from the measured spectrum. The contribution of the $2\nu\beta\beta$ decay to the residual spectrum is clearly visible. Its half-life was determined under the assumption that the entire residual spectrum is composed of the $2\nu\beta\beta$ signal. Due to non-identified background in the energy region below 700 keV, the fit interval for the $2\nu\beta\beta$ signal is chosen between 700–2040 keV. With the above assumption, this region contains 64553 $2\nu\beta\beta$ events, corresponding to 51.7% of the total $2\nu\beta\beta$ signal.

The theoretically expected $2\nu\beta\beta$ spectrum was fitted to the data in a maximum likelihood fit with $T_{1/2}$ as free parameter, resulting in the following half-life for the $2\nu\beta\beta$ decay at 68% C.L. (combined result for the five detectors):

$$T_{\frac{1}{2}}^{2\nu} = \left(1.55 \pm 0.01(\text{stat}) \, {}^{+0.19}_{-0.15}(\text{syst}) \right) \times 10^{21} \, \text{y} \, . \qquad (4)$$

The statistical error is evaluated from the parabolic behaviour of the logarithmic likelihood ratio which corresponds to a χ^2 function. The systematic error includes the error of the simulated detector response, the error made by the misplacement of background activities and the normalization error due to the statistical error of the measured γ lines (see [17]).

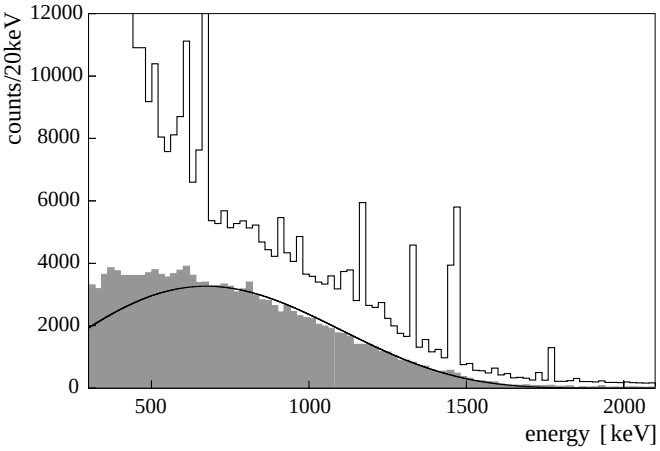

Fig. 3. Summed spectra of all five detectors after 47.7 kg y of measurement together with the residual spectrum after subtracting all identified background components. The thick line shows the fitted $2\nu\beta\beta$ signal.

The inferred value for the half-life is consistent with earlier results of this experiment [15,23] and with the result of [24] (but *not* with the result of [25]) —as well as with the range of theoretical predictions, which lie between 1.5×10^{20}–2.99×10^{21} y [26–30]. The prediction of [26,30] for the $2\nu\beta\beta$ matrix element agrees within a factor of $\sqrt{2}$ with the experimental value. This calculation, *underestimating* the matrix element by 40%, was the best theoretical *prediction* of the various matrix element calculations for two-neutrino $\beta\beta$ decay of ^{76}Ge.

The half-life limits of the majoron-emitting decay modes were determined from the same data set by fitting the $2\nu\beta\beta$ and the $0\nu\chi\beta\beta$ spectra simultaneously. The considered majoron models are described in [31]. Since the selected energy interval starts at 700 keV, an analysis of the decay-mode with the spectral index $n = 7$ (maximum at about 500 keV) was not possible. The results of the fits for $n = 1$ and $n = 3$ are shown in table 2. The $2\nu\beta\beta$ half-lives extracted in the two-parameter fits are consistent within 1σ with the exclusive double beta decay evaluation. In table 3 a comparison of the effective majoron-neutrino couplings extracted for different double beta nuclei is made.

5 Results for the $0\nu\beta\beta$ decay

For the evaluation of the $0\nu\beta\beta$ decay we consider the raw data of all five detectors as well as data with pulse shape analysis. The pulse shape analysis method used here is described elsewhere [32]. No further data manipulation is done, *e.g.* the previously established background model is not subtracted. We see in none of the two data sets an indication for a peak at the Q-value of 2038.56 ± 0.32 keV [33] of the $0\nu\beta\beta$ decay.

The total spectrum of the five detectors with a statistical significance of 53.9 kg y contains all the data with the exception of the first 200 d of measurement of each

Table 2. Half-life limits for the majoron-emitting decay modes and derived coupling constants using the matrix elements from [31] for different majoron models (n is the spectral index of the decay mode).

Modus	Model	n	$T_{1/2}^{0\nu\chi} >$ (90% C.L.)	$\langle g_{\nu\chi}\rangle <$ (90% C.L.)
$\chi\beta\beta$	[34]	1	6.4×10^{22} y	8.1×10^{-5}
$l\chi\beta\beta$	[35],[36]	3	1.4×10^{22} y	0.11 (0.04)

Table 3. Half-life limits on the majoron-emitting decay mode $0\nu\chi\beta\beta$ extracted from different nuclei and the derived limits on the effective majoron-neutrino coupling for $n = 1$.

Nucleus	Reference	$T_{1/2}^{0\nu\chi} >$	$\langle g_{\nu\chi}\rangle <$	C.L. (%)
^{76}Ge	this work	6.4×10^{22} y	8.1×10^{-5}	90
^{82}Se	[37]	2.4×10^{21} y	2.3×10^{-4}	90
^{96}Zr	[38]	3.5×10^{20} y	2.6×10^{-4}	90
^{100}Mo	[39]	5.4×10^{21} y	7.3×10^{-5}	68
^{116}Cd	[40]	3.7×10^{21} y	1.2×10^{-4}	90
^{128}Te	[41]	7.7×10^{24} y	3.0×10^{-5}	90
^{136}Xe	[42]	7.2×10^{21} y	2.0×10^{-4}	90
^{150}Nd	[43]	2.8×10^{20} y	9.9×10^{-5}	90

detector, because of possible interference with the cosmogenic ^{56}Co. The interpolated energy resolution at the energy at the hypothetical $0\nu\beta\beta$ peak is (4.23 ± 0.14) keV. The expected background in the $0\nu\beta\beta$ region is estimated from the energy interval 2000–2080 keV. In this range the background is (0.19 ± 0.01) counts/(kg y keV). The expected background in the 3σ peak interval, centered at 2038.56 keV interpolated from the adjacent energy regions, is (110.3 ± 3.9) events. The number of measured events in the same peak region is 112. To extract a half-life limit for the $0\nu\beta\beta$ decay we follow the conservative procedure recommended in [44].

With the achieved energy resolution, the number of excluded events in the 3σ peak region is 19.8 (12) with 90% C.L. (68% C.L.), resulting in a half-life limit of (for the $0^+ \to 0^+$ transition):

$$T_{1/2}^{0\nu} \geq 1.3 \times 10^{25} \text{ y} \quad 90\% \text{ C.L.},$$
$$T_{1/2}^{0\nu} \geq 2.2 \times 10^{25} \text{ y} \quad 68\% \text{ C.L.}.$$

We consider now the data for which the pulse shape of each interaction of the detectors was recorded and analyzed. The total statistical significance is 35.5 kg y and the background index in the energy region between 2000–2080 keV is (0.06 ± 0.01) events/(kg y keV), about a factor 3 lower than for the full data set. This is due to the large fraction of multiple Compton scattered events in this energy region, which are effectively suppressed by the pulse shape discrimination method. The expected number of events from the background left and right of the peak region is (20.4 ± 1.6) events, the measured number of events in the 3σ peak region is 21. Following again the method proposed by [44], we can exclude 9.3 (5.5) events with

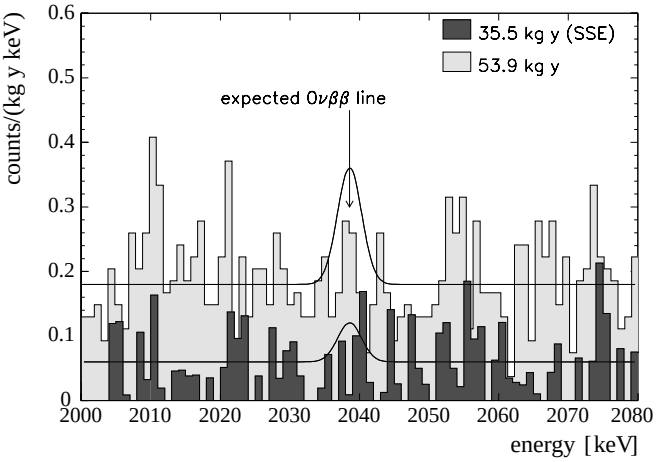

Fig. 4. Sum spectrum of all five detectors with 53.9 kg y and SSE spectrum with 35.5 kg y in the region of interest for the $0\nu\beta\beta$ decay. The curves correspond to the excluded signals with $T_{1/2}^{0\nu} \geq 1.3 \times 10^{25}$ y (90% C.L.) and $T_{1/2}^{0\nu} \geq 1.9 \times 10^{25}$ y (90% C.L.), respectively.

90% C.L. (68% C.L.). The limit on the half-life is:

$$T_{1/2}^{0\nu} \geq 1.9 \times 10^{25} \text{ y} \quad 90\% \text{ C.L.},$$
$$T_{1/2}^{0\nu} \geq 3.1 \times 10^{25} \text{ y} \quad 68\% \text{ C.L.}^{1}.$$

To examine the dependence of the half-life limit on the position of the 3σ peak interval (12.7 keV) in the spectrum, we shifted the peak interval between 2028 keV and 2048 keV. It results in a variation of the half-life limit between 2.5×10^{25} y and 1.2×10^{25} y at 90% C.L. (for the data with pulse shape analysis). This demonstrates a rather smooth background in the considered energy region. Figure 4 shows the combined spectrum of the five detectors after 53.93 kg y and the spectrum of point-like interactions, corrected for the detection efficiency, after 35.5 kg y. The solid lines represent the exclusion limits for the two spectra at the 90% C.L. Using the matrix elements of [30] and neglecting right-handed currents, we can convert the lower half-life limit into an upper limit on the effective Majorana-neutrino mass, which are listed in table 4. As mentioned in sect. 4, the calculation [30] used here, gave the prediction most close to the experimental 2ν

[1] These limits are slightly sharpened when the new Q-value of 2039.006(50) keV is used, which has been published [45] after finalizing this paper.

Table 4. Limits on the effective Majorana-neutrino mass from the $0\nu\beta\beta$ decay of ^{76}Ge calculated with the matrix elements from [30].

	$T^{0\nu}_{1/2} >$	$\langle m \rangle <$	C.L. (%)
Full data set	1.3×10^{25} y	0.42 eV	90
	2.2×10^{25} y	0.33 eV	68
SSE data	1.9×10^{25} y	0.35 eV	90
	3.1×10^{25} y	0.27 eV	68

decay half-life. It underestimates the 2ν matrix elements by 40%, and thus will also *underestimate* (to a smaller extent) the matrix element for 0ν decay and thus lead to, within this calculation, a corresponding *overestimate* of the neutrino mass limit.

There are other calculations of 0ν decay giving more "optimistic" (lower) values for the mass limit [46,47], and others, giving still larger limits [48–50] (see the discussion in [51].) It might be mentioned, that the calculation of [49] still does not use a realistic nucleon-nucleon force, those using "large-scale" shell model calculations [48], use too small a configuration space (leaving out important spin orbit partners), and also the calculations of [50] do not fulfill the Ikeda sum rule.

For a more detailed discussion of the status of matrix elements we refer to [4,50,52,53]. From the latter works, in particular also the one using the Second-Quasi Random Phase Approximation Method [53] it can be concluded that the uncertainty of the deduced mass limit is not larger than 50%.

The HEIDELBERG-MOSCOW experiment is presently giving the most stringent upper limit on the Majorana-neutrino mass, of 0.35 eV at 90% C.L. (0.27 eV at 68% C.L.). The values quoted in a previous paper [51], with a statistical significance of 24.2 kg y of data with pulse shape analysis, were 0.2 eV for the mass limit and 0.38 eV for the sensitivity of the experiment (both at 90% C.L.), after the recommendation of [54]. Thus, not unexpected, after additional 11.3 kg y of statistics, the limit on the effective neutrino mass approached the experimental sensitivity, as defined in [55]. The second best limit at present comes from the half-life limit for decay of ^{128}Te measured in a geochemical experiment [56,57] and is 1.1 eV (with matrix elements of [30]). The third best experimental limit is coming at present from the cryogenic ^{130}Te experiment of the Milano group yielding a half-life limit of 1.6×10^{23} y [58], corresponding to a mass limit of $<$ 1.7 eV (with the matrix element from [30]. There is also a second Germanium experiment (IGEX) which has closed operation by the end of 1999 [59] and which has results statistically inferior to the results presented here [60,61]. Analysing the data given in [60, 61] in the same conservative way as applied in this paper leads to a half-life limit of 0.55×10^{25} y (corresponding, with the matrix elements of [30], to $\langle m \rangle < 0.7$ eV). It has to be kept in mind, however, that in this experiment some unclear data selection seems to be made. A "visual technique" of pulse shape discrimination is applied [61].

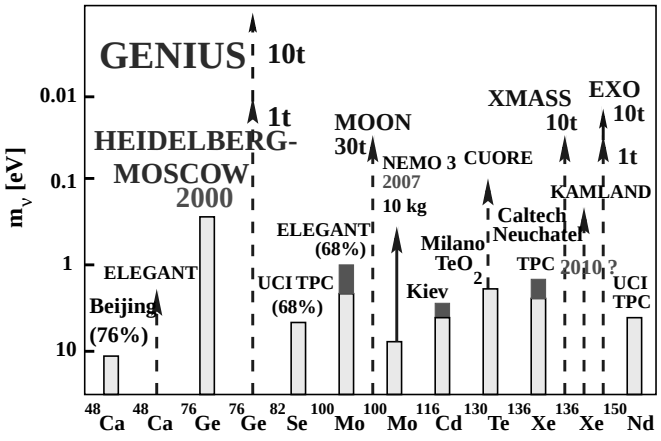

Fig. 5. Present situation, and the expectation for the future, of the most promising $\beta\beta$ experiments. Light parts of the bars: present status; dark parts: expectation for running experiments; solid and dashed lines: experiments under construction and proposed experiments, respectively (from [62], see also [63,64]).

6 Summary and discussion

We performed an analysis of the most recent data of the HEIDELBERG-MOSCOW double beta decay experiment. The data of the complete setup with five enriched ^{76}Ge detectors, with a total statistical significance of 47.4 kg y, were analyzed with respect to the two-neutrino and majoron-emitting decay modes for the first time. A Monte Carlo simulation based on a modified version of GEANT3.21 was performed in order to identify the most significant background sources and to establish a quantitative background model. The theoretical shapes of the $2\nu\beta\beta$ and $0\nu\chi\beta\beta$ decay spectra were fitted in a maximum likelihood fit to the resulting spectrum after subtraction of the background model from the measured, summed spectrum of all detectors. The low-energy background of the HEIDELBERG-MOSCOW experiment requires further investigation. A possible background source not taken into account so far could be surface contaminations of the crystal and/or copper parts of the cryostats with ^{210}Pb, which is produced and accumulated by the decay of ^{222}Rn. This and other potential background sources will be implemented in a new Monte Carlo simulation using GEANT4 [65]. A more complete background model will allow to determine the half-life of the $2\nu\beta\beta$ decay with still higher precision.

The resulting half-life for the $2\nu\beta\beta$ decay confirms our previous measurement and confirms theoretical expectations [26,30] within a factor of two (a factor of $\sqrt{2}$ in the matrix element). No evidence for a majoron-accompanied decay or for the neutrinoless decay was observed. The upper limit on the effective Majorana-neutrino mass of 0.35 eV (0.27 eV) (using the matrix elements of [30]) is the worldwide most stringent limit —the HEIDELBERG-MOSCOW experiment is keeping this position of the most sensitive $\beta\beta$ experiment for eight years now already. In fig. 5 this value from the HEIDELBERG-MOSCOW ex-

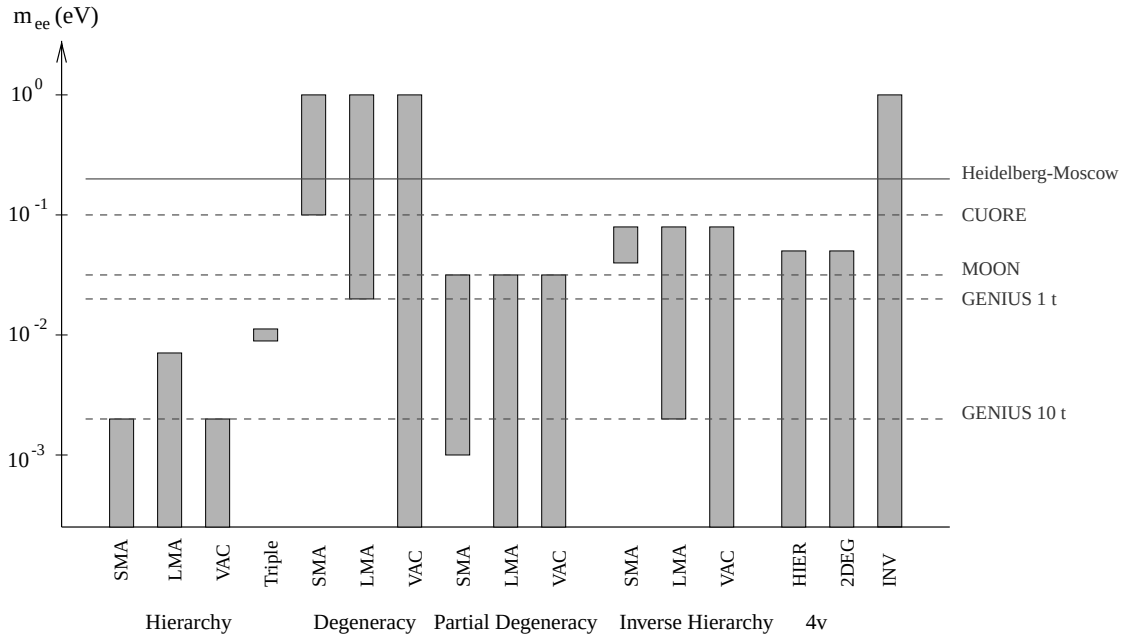

Fig. 6. Ranges of the effective Majorana-neutrino mass allowed from all present neutrino oscillation experiments, for several neutrino mass scenarios, compared to our present limit (solid line) and to the potential of planned future $\beta\beta$ experiments (dashed lines) (see [1,2,4,62–64]).

periment is compared with limits of the most sensitive other $\beta\beta$ experiments. With this result for the limit of the effective Majorana-neutrino mass double beta experiments start to enter into the range to give a serious contribution to the neutrino mass matrix (fig. 6).

In degenerate models we can conclude from the experimental bound an upper limit on the common neutrino mass eigenvalue. For the Large Mixing Angle (LMA) MSW solution of the solar-neutrino problem we obtain $m_{1,2,3} < 1.1\,\mathrm{eV}$, implying $\sum_i m_i < 3.2\,\mathrm{eV}$ [1,2,62]. This first number is sharper than what has recently been obtained from tritium ($m < 2.2\,\mathrm{eV}$), and the second is sharper than the limit $\sum_i m_i < 5.5\,\mathrm{eV}$ still compatible with most recent fits of Cosmic Microwave Background radiation and Large Scale Structure data (see *e.g.* [66]). The present sensitivity of the HEIDELBERG-MOSCOW experiment probes cosmological models including hot dark matter, for the range of small mixing angles, already now on a level of future satellite experiments MAP and PLANCK (see [1,2]). It is of interest also for new *Z-burst* models recently discussed as explanation for super-high-energy cosmic ray events beyond the GZK cutoff [67,68].

The result for $\langle m \rangle$ from the HEIDELBERG-MOSCOW experiment has found large resonance. It has been shown that it excludes for example the Small Mixing Angle MSW solution of the solar neutrino problem in degenerate scenarios, if neutrinos are considered as hot dark matter in the Universe [69–71]. This conclusion has been drawn, before the Superkamiokande collaboration presented their evidence for exclusion of the SMA MSW solution, in June 2000.

If future searches will show that $m_\nu > 0.1\,\mathrm{eV}$, then the three-neutrino mass schemes, which will survive, are those with neutrino mass degeneracy, and from the four-neutrino schemes, investigated in [1], those with inverse mass hierarchy will survive (see fig. 6 and [1,2,62]). A substantial increase in sensitivity of double beta experiments beyond this level, requires new experimental approaches, making use of much higher source strength and drastically reduced background. This could be accomplished by our proposed GENIUS project [72] which, operating 0.1-10 t of enriched ^{76}Ge directly in ultrapure liquid nitrogen, could test the effective Majorana-neutrino mass down to 0.01 or even 0.002 eV.

References

1. H.V. Klapdor-Kleingrothaus, H. Päs, A.Y. Smirnov, hep-ph/0003219, (2000); Phys. Rev. D **63**, 073005 (2001).
2. H.V. Klapdor-Kleingrothaus, H. Päs, A.Y. Smirnov hep-ph/0103076, in *Proceedings of DARK2000, Heidelberg, 10-15 July, 2000, Germany*, edited by H.V. Klapdor-Kleingrothaus (Springer, Heidelberg, 2001) pp. 420-434.
3. H.V. Klapdor-Kleingrothaus, in *Neutrino Physics*, edited by K. Winter (Cambridge University Press, 2000) pp. 113-127.
4. H.V. Klapdor-Kleingrothaus, *60 Years of Double Beta Decay – From Nuclear Physics to Beyond the Standard Model* (World Scientific, Singapore, 2001).
5. P. Vogel, in *Current Aspects of Neutrino Physics*, edited by D.O. Caldwell (Springer Verlag, 2001).
6. M. Hirsch, H.V. Klapdor-Kleingrothaus, S.G. Kovalenko, Phys. Rev. D **53**, 1329 (1996).

7. M. Hirsch, H.V. Klapdor-Kleingrothaus, S.G. Kovalenko, Phys. Rev. D **57**, 2020 (1998).
8. M. Hirsch, H.V. Klapdor-Kleingrothaus, S.G. Kovalenko, Phys. Lett. B **378**, 17 (1996).
9. H.V. Klapdor-Kleingrothaus, H. Päs, U. Sarkar, Eur. Phys. J. A **5**, 3 (1999).
10. O. Panella *et. al.*, Phys. Rev. D **62**, 015013 (2000).
11. H.V. Klapdor-Kleingrothaus, Int. J. Mod. Phys. A **13**, 3953 (1998).
12. H.V. Klapdor-Kleingrothaus, in *Proceedings of the First International Symposium on Lepton and Baryon Number Violation (LEPTON-BARYON 1998), Trento, Italy, April 1998*, edited by H.V. Klapdor-Kleingrothaus, I.V. Krivosheina (IOP, Bristol and Philadelphia, 1999) pp. 251-301.
13. H.V. Klapdor-Kleingrothaus, Springer Tracts Mod. Phys., Vol. **163**, (2000) pp. 69-104.
14. P. Bamert, C.P. Burgess, R.N. Mohapatra, Nucl. Phys. B **449**, 25 (1995).
15. HEIDELBERG-MOSCOW Collaboration, Phys. Rev. D **55**, 54 (1997).
16. HEIDELBERG-MOSCOW Collaboration, Phys. Rev. D **59**, 022001 (1998).
17. A. Dietz, Diploma thesis, University of Heidelberg (1999) unpublished.
18. Nuclear Data Sheets (Academic Press, Duluth, MN).
19. MACRO Collaboration (C. deMarzo), Nucl. Instrum. Methods A **314**, 380 (1992).
20. P. Belli *et al.*., Nuovo Cimento A **101**, 959 (1989).
21. C. Zeitnitz, T.A. Gabriel, *The GEANT-Calor Interface*, in *Proceedings of the 3rd International Conference on Calorimetry in High Energy Physics* (World Scientific, 1993) p. 394.
22. E. Pernicka, private communication (1993).
23. HEIDELBERG-MOSCOW Collaboration, Phys. Lett. B **322**, 176 (1994).
24. A. Morales, Nucl. Phys. Proc. Suppl. **77**, 335 (1999).
25. F.T. Avignone et al., Phys. Lett. B **256**, 559 (1991).
26. K. Muto, E. Bender, H.V. Klapdor, Z. Phys. A **334**, 177 (1989).
27. E. Caurier *et al.*, Phys. Rev. Lett. **77**, 1954 (1996).
28. J. Engel *et al.*, Phys. Rev. C **37**, 731 (1988).
29. X.R. Wu *et al.*, Phys. Lett. B **272**, 169 (1991); **276**, 274 (1992).
30. A. Staudt, K. Muto, H.V. Klapdor-Kleingrothaus, Europhys. Lett. **13**, 31 (1990).
31. M. Hirsch, H.V. Klapdor-Kleingrothaus, S. Kovalenko, H. Päs, Phys. Lett. B **372**, 8 (1996).
32. J. Hellmig, H.V. Klapdor-Kleingrothaus, Nucl. Instrum. Methods A **445**, 638 (2000).
33. J.G. Hykawy *et. al.*, Phys. Rev. Lett. **67**, 1708 (1991).
34. Y. Chikashige, R.N. Mohapatra, R.D. Peccei, Phys. Rev. Lett. **45**, 1926 (1980); Phys. Lett. B **98**, 265 (1981).
35. C.P. Burgess, J.M. Cline, Phys. Lett. B **298**, 141 (1993); Phys. Rev. D **49**, 5925 (1994).
36. C.D. Carone, Phys. Lett. B **308**, 85 (1993).
37. NEMO Collaboration (R. Arnold *et al.*), Nucl. Phys. A **636**, 209 (1998).
38. NEMO Collaboration (R. Arnold *et al.*), Nucl. Phys. A **658**, 299 (1999).
39. H. Ejiri *et al.*, Nucl. Phys. A **611**, 85 (1996).
40. F.A. Danevich *et al.*, Phys. Rev. C **62**, 045501 (2000).
41. T. Bernatowicz et al., Phys. Rev. Lett. **69**, 2341 (1992).
42. Caltech-PSI-Neuchatel Collaboration (R. Luescher), Nucl. Phys. B Proc. Suppl. **66**, 195 (1998).
43. A. De Silva *et al.*, Phys. Rev. C **56**, 2451 (1997).
44. PDG 96 (R.M. Barnett *et al.*), Phys. Rev. D **54**, 1 (1996).
45. G. Douysset *et al.*, Phys. Rev. Lett. **86**, 4259 (2001).
46. T. Tomoda, Rep. Progr. Phys. **54**, 53 (1991).
47. W.C. Haxton, G.J. Stephenson, Progr. Part. Nucl. Phys. **12**, 409 (1984).
48. E. Caurier *et al.*, Phys. Rev. Lett. **77**, 1954 (1996).
49. J. Engel *et al.*, Phys. Rev. C **37**, 731 (1988).
50. F. Simkovic *et al.*, Phys. Lett. B **393**, 267 (1997).
51. HEIDELBERG-MOSCOW Collaboration, Phys. Rev. Lett. **83**, 41 (1999).
52. S. Stoica, H.V. Klapdor-Kleingrothaus, Nucl. Phys. A **694**, 269 (2001).
53. S. Stoica, H.V. Klapdor-Kleingrothaus, Eur. Phys. J. A **9**, 345 (2000).
54. PDG 98 (C. Caso *et al.*), Eur. Phys. J. C **3**, 1 (1998).
55. G.J. Feldman, R.D. Cousins, Phys. Rev. D **57**, 3873 (1998).
56. T. Bernatowicz *et al.*, Phys. Lett. **69**, 2341 (1992).
57. T. Bernatowicz *et al.*, Phys. Rev. C **47**, 806 (1993).
58. E. Fiorini, March 2001, Gran Sasso Scientific Community, private communication.
59. I.V. Kirpichnikov, June 2000, *Neutrino2000*, private communication.
60. D. Gonzales et al., Nucl. Phys. Proc. Suppl. **87**, 278 (2000).
61. C.E. Aalseth *et al.*, in *Proceedings of NANP'99*, edited by V. Bednjakov *et al.*, Yad. Fiz. **63**, N. 7, 1299 (2000).
62. H.V. Klapdor-Kleingrothaus, in *Proceedings of NANPino 2000, International conference on NON-Accelerator New Physics in neutrino observations, Dubna, Russia, July 2000*, hep-ph/0102319 and `http://www.mpi-hd.mpg.de/non_acc/Talks.html`.
63. E. Fiorini, Phys. Rep. **307**, 309 (1998).
64. A. Bettini, Nucl. Phys. B Proc. Suppl. **100**, 332 (2001).
65. `http://wwwinfo.cern.ch/asd/geant4/geant4.html`.
66. M. Tegmark *et. al.*, hep-ph/0008145.
67. T.J. Weiler, Astropart. Phys. **11**, 303 (1999); *Proceedings of Beyond The Desert 1999, Second International Conference on Particle Physics Beyond the Standard Model, Castle Ringberg, Germany, June 1999*, edited by H.V. Klapdor-Kleingrothaus, I.V. Krivosheina (IOP, Bristol, 2000) p. 1085.
68. H. Päs, T.J. Weiler, hep-ph/0101091.
69. G. Georgi, S.L. Glashow, Phys. Rev. D **61**, 097301 (2000).
70. H. Minakata, O. Yasuda, Phys. Rev. D **56**, 1632 (1997).
71. H. Minakata, hep-ph/0004249.
72. H.V. Klapdor-Kleingrothaus, in *Proceedings of Beyond The Desert 1997, First International Conference on Particle Physics Beyond the Standard Model, Castle Ringberg, Germany, June 1997*, edited by H.V. Klapdor-Kleingrothaus, H. Päs (IOP, Bristol, 1998) pp. 485–531; H.V. Klapdor-Kleingrothaus, J. Hellmig, M. Hirsch, J. Phys. G **24**, 483 (1998); H.V. Klapdor-Kleingrothaus *et.al.*, hep-ph/9910205 and in *Proceedings of Beyond The Desert 1999, Second International Conference on Particle Physics Beyond the Standard Model, Castle Ringberg, Germany, June 1999*, edited by H.V. Klapdor-Kleingrothaus, I.V. Krivosheina (IOP, Bristol, 2000) pp. 915-1014.